Chapter 1

Fluctuations and Correlations in Chemical Reaction Kinetics and Population Dynamics

Uwe C. Täuber

Department of Physics (MC 0435) and
Center for Soft Matter and Biological Physics, Virginia Tech,
850 West Campus Drive, Blacksburg, VA 24061, USA
tauber@vt.edu

This chapter provides a pedagogical introduction and overview of spatial and temporal correlation and fluctuation effects resulting from the fundamentally stochastic kinetics underlying chemical reactions and the dynamics of populations or epidemics. After reviewing the assumptions and mean-field type approximations involved in the construction of chemical rate equations for uniform reactant densities, we first discuss spatial clustering in birth-death systems, where non-linearities are introduced through either density-limiting pair reactions, or equivalently via local imposition of finite carrying capacities. The competition of offspring production, death, and non-linear inhibition induces a population extinction threshold, which represents a non-equilibrium phase transition that separates active from absorbing states. This continuous transition is characterized by the universal scaling exponents of critical directed percolation clusters. Next we focus on the emergence of depletion zones in single-species annihilation processes and spatial population segregation with the associated reaction fronts in two-species pair annihilation. These strong (anti-)correlation effects are dynamically generated by the underlying stochastic kinetics. Finally, we address noise-induced and fluctuation-stabilized spatio-temporal patterns in basic predator-prey systems, exemplified by spreading activity fronts in the two-species Lotka–Volterra model as well as spiral structures in the May–Leonard variant of cyclically competing three-species systems akin to rock-paper-scissors games.

1. Introduction

The kinetics of chemical reactions, wherein the identity or number of reactant particles changes either spontaneously or upon encounter, constitutes a highly active research field in non-equilibrium statistical physics of stochastically interacting particle systems, owing both to the fundamental questions it addresses as well as its broad range of applications. Of specific interest are reaction-diffusion models that for example capture chemical reactions on catalytic solid surfaces or in gels where convective transport is inhibited. This scenario of course naturally pertains to genuine reactions in chemistry or biochemistry, and in nuclear, astro-, and particle physics. Yet reaction-diffusion models are in addition widely utilized for the quantitative description of a rich variety of phenomena in quite distinct disciplines that range from population dynamics in ecology, growth and competition of bacterial colonies in microbiology, the dynamics of topological defects in the early universe in cosmology, equity and financial markets in economics, opinion exchange and the formation of segregated society factions in sociology, and many more. Reactive 'particles' also emerge as relevant effective degrees of freedom in other physical applications; prominent examples include excitons kinetics in organic semiconductors, domain wall interactions in magnets, and interface dynamics in stochastic growth models.

The traditional textbook literature, e.g., in physical chemistry and mathematical biology, almost exclusively focuses on a description of reacting particle systems in terms of coupled deterministic non-linear rate equations. While these certainly represent an indispensable tool to characterize such complex dynamical systems, they are ultimately based on certain mean-field approximations, usually involving the factorization of higher moments of stochastic variables in terms of products of their means, as in the classical Guldberg–Waage law of mass action. Consequently, both temporal and spatial correlations are neglected in such treatments, and are in fact also only rudimentarily captured in standard spatial extensions of the mean-field rate equations to reaction-diffusion models. Under non-equilibrium conditions, however, spatio-temporal fluctuations often play a quite significant role and may even qualitatively modify the dynamics, as has been clearly established over the past decades through extensive Monte Carlo computer simulations, a remarkable series of exact mathematical treatments (albeit mostly in one dimension), and a variety of insightful approximative analytical schemes that extend beyond mean-field theory. These include mappings of the stochastic dynamics to effective field theo-

ries and subsequent analysis by means of renormalization group methods.

In the following, we shall discuss the eminent influence of spatio-temporal fluctuations and self-generated correlations in five rather simple particle reaction and, in the same general language, population ecology models that however display intriguing non-trivial dynamical features:

(1) As in thermal equilibrium, strong fluctuations and long-range correlations emerge in the vicinity of continuous phase transitions between distinct non-equilibrium steady states, as we shall exemplify for the extinction threshold that separates and active from an absorbing state. In this paradigmatic situation, the dynamical critical properties are described by the scaling exponents of critical directed percolation clusters which assume non-mean-field values below the critical dimension $d_c = 4$.

(2) Crucial spatio-temporal correlations may also be generated by the chemical kinetics itself; this is indeed the case for simple single-species pair annihilation reactions that produce long-lived depletion zones in dimensions $d \leq 2$ which in turn slow down the resulting algebraic density decay.

(3) For two-species binary annihilation, the physics becomes even richer: for $d \leq 4$, particle anti-correlations induce species segregation into chemically inert, growing domains, with the reactions confined to their interfaces.

(4) Spatially extended stochastic variants of the classical Lotka–Volterra model for predator-prey competition and coexistence display remarkably rich noise-generated and -stabilized dynamical structures, namely spreading activity fronts that lead to erratic but persistent population oscillations.

(5) Cyclic competition models akin to the rock-paper-scissors game too produce intriguing spatio-temporal structures, whose shape is determined in a subtle manner by the presence or absence of conservation laws in the stochastic dynamics: Three species subject to cyclic Lotka–Volterra competition with conserved total particle number organize into fluctuating clusters, whereas characteristic spiral patterns form in the May–Leonard model with distinct predation and birth reactions.

2. Chemical Master and Rate Equations

2.1. *Stochastic reaction processes*

To begin, we consider simple *death-birth* reactions,[1–5] with reactants of a single species A either spontaneously decaying away or irreversibly reaching a chemically inert state $\emptyset$: $A \to \emptyset$ with rate μ; or producing identical offspring particles, e.g.: $A \to A + A$ with rate σ. Note that we may also

view species A as indicating individuals afflicted with a contagious disease from which they may recover with rate μ or that they can spread among others with rate σ. We shall consider these reactions as continuous-time Markovian stochastic processes that are fully determined by prescribing the transition rates from any given system configuration at instant t to an infinitesimally later time $t + dt$. Assuming mere local processes, i.e., for now ignoring any spatial degrees of freedom, our reaction model is fully characterized by specifying the number n of particles or individuals of species A at time t. The death-birth reactions are then encoded in the transition rates $w(n \to n-1) = \mu\, n$ and $w(n \to n+1) = \sigma\, n$ that linearly depend on the instantaneous particle number n. Accounting for both gain and loss terms for the configurational probability $P(n,t)$ then immediately yields the chemical *master equation*[1,4–7]

$$\left.\frac{\partial P(n,t)}{\partial t}\right|_{\rm db} = \mu\,(n+1)\,P(n+1,t) - (\mu+\sigma)\,n\,P(n,t) + \sigma\,(n-1)\,P(n-1,t)\ . \tag{1}$$

This temporal evolution of the probability $P(n,t)$ directly transfers to its moments $\langle n(t)^k \rangle = \sum_{n=0}^{\infty} n^k\, P(n,t)$. For example, for the *mean particle number* $a(t) = \langle n(t) \rangle$, a straightforward summation index shift results in the exact linear differential equation

$$\begin{aligned}\left.\frac{\partial a(t)}{\partial t}\right|_{\rm db} &= \sum_{n=1}^{\infty} n\,\left.\frac{\partial P(n,t)}{\partial t}\right|_{\rm db} \\ &= \sum_{n=1}^{\infty} \left[\mu\, n(n-1) - (\mu+\sigma)\, n^2 + \sigma\, n(n+1)\right] P(n,t) = (\sigma-\mu)\, a(t)\ ,\end{aligned} \tag{2}$$

as the terms $\sim n^2$ in the bracket all cancel. Its solution $a(t) = a(0)\, e^{(\sigma-\mu)t}$ naturally indicates that if the particle decay rate is faster than the birth rate, $\mu > \sigma$, the population will go extinct and reach the inactive, *absorbing* empty state $a = 0$, whereupon all reactions irretrievably cease. In stark contrast, Malthusian exponential population explosion ensues for $\sigma > \mu$.

In order to prevent an unrealistic population divergence, one may impose a non-linear process that effectively limits the reactant number; for example, we could add coagulation $A + A \to A$ with reaction rate λ that can be viewed as mimicking constraints imposed by locally restricted resources. In the context of disease spreading, this scenario is often referred to as *simple epidemic process*. The frequency of such binary processes annihilating one of the reactants is proportional to the number of particle pairs in the system, whence the associated transition rate becomes

$w(n \to n-1) = \lambda\, n(n-1)$, and the master equation reads[4,5,8,9]

$$\left.\frac{\partial P(n,t)}{\partial t}\right|_{\rm an} = \lambda\left[n(n+1)\,P(n+1,t) - n(n-1)\,P(n,t)\right] . \tag{3}$$

Proceeding as before, one now finds for the mean particle number decay

$$\left.\frac{\partial a(t)}{\partial t}\right|_{\rm an} = \lambda \sum_{n=1}^{\infty}\left[n(n-1)^2 - n^2(n-1)\right] P(n,t) = -\lambda\,\langle [n(n-1)](t)\rangle\ . \tag{4}$$

As to be expected, it is governed by the instantaneous number of particle pairs; that quantity involves the second moment $\langle n(t)^2\rangle$, whose time evolution in turn is determined by the third moment, etc. Consequently, one faces an infinite hierarchy of moment differential equations that is much more difficult to analyze than the simple closed Eq. (2).

2.2. *Mean-field rate equation approximation*

A commonly applied scheme to close the moment hierarchy for non-linear stochastic processes is to impose a mean-field type factorization for higher moments. The simplest such approximation entails neglecting any fluctuations, setting the connected two-point correlation function to zero, $C(t,t') = \langle n(t)\,n(t')\rangle - \langle n(t)\rangle\langle n(t')\rangle \approx 0$. This assumption should hold best for large populations $n \gg 1$, when relative mean-square fluctuations $(\Delta n)^2/\langle n\rangle^2 = C(t,t)/a(t)^2$ should be small; Eq. (4) then simplifies to the kinetic *rate equation*

$$\left.\frac{\partial a(t)}{\partial t}\right|_{\rm an} \approx -\lambda\, a(t)^2\ , \tag{5}$$

or $\partial a(t)^{-1}/\partial t \approx \lambda$. It is readily integrated to $a(t)^{-1} = a(0)^{-1} + \lambda\, t$, i.e.,

$$a(t) = \frac{a(0)}{1 + \lambda\, a(0)\, t}\ , \tag{6}$$

which becomes independent of the initial particle number $a(0)$ and decays to zero algebraically $\sim 1/\lambda\, t$ for large times $t \gg 1/\lambda\, a(0)$. Note that the right-hand side of the rate equations resulting from mean-field factorizations of non-linear reaction terms encode the corresponding stochiometric numbers as powers of the reactant numbers, precisely as in the Guldberg–Waage law of mass action describing reaction concentration products in chemical equilibrium.[5,7] Already in non-spatial systems, these factorizations disregard any temporal fluctuations; in spatially extended systems, they moreover assume well-mixed and thus homogeneously distributed reactants.

3. Population Dynamics with Finite Carrying Capacity

3.1. *Mean-field rate equation analysis*

Next we combine the three reaction processes of the preceding section to arrive at the simplest possible population dynamics model for a single species that incorporates death with rate μ, (asexual) reproduction with rate σ, and (non-linear) competition with rate λ to constrain the active-state particle number.[2,3] Adding the right-hand sides of Eqs. (2) and (5) yields the associated mean-field rate equation for the particle number or population:

$$\frac{\partial a(t)}{\partial t} \approx (\sigma - \mu)\, a(t) - \lambda\, a(t)^2 = \lambda\, a(t)\, [r - a(t)] \ . \tag{7}$$

In the last step we have cast the rate equation in the form of a *logistic model* with *carrying capacity* $r = (\sigma - \mu)/\lambda$. Its stationary solutions are the absorbing state $a = 0$ and a population number equal to the carrying capacity $a = r$. Straightforward linear stability analysis of Eq. (7) establishes that the latter stationary state is approached for $\sigma > \mu$ or $r > 0$, whereas of course $a(t) \to 0$ for $\sigma < \mu$ ($r < 0$).

For $\sigma \neq \mu$, the ordinary first-order differential equation (7) is readily integrated after variable separation:

$$\lambda\, t = \frac{1}{r} \int_{a(0)}^{a(t)} \left(\frac{1}{a} + \frac{1}{r-a} \right) da = \frac{1}{r}\, \ln \left[\frac{a(t)}{a(0)}\, \frac{r - a(0)}{r - a(t)} \right] .$$

Solving for the particle number at time t gives

$$a(t) = \frac{a(0)}{e^{(\mu-\sigma)t}\, [1 - a(0)/r] + a(0)/r} \ . \tag{8}$$

As anticipated, this results in exponential decay for $\mu > \sigma$ with characteristic time $\tau = 1/|\mu - \sigma| = 1/\lambda\, |r|$; in the active state, the particle number also approaches the carrying capacity r exponentially with rate $1/\tau$, and monotonically from above or below for $a(0) > r$ and $a(0) < r$, respectively. Right at the extinction threshold $\sigma = \mu$ ($r = 0$) separating the active and inactive and absorbing states, Eq. (7) reduces to Eq. (5) for pair annihilation, and hence the exponential kinetics of Eq. (8) is replaced by the power law decay (6), as follows also from taking the limit $\mu - \sigma \to 0$ in Eq. (8).

3.2. *Diffusive spreading and spatial clustering*

At least in a phenomenological manner, the above analysis can be readily generalized to spatially extended systems by adding (e.g., unbiased

nearest-neighbor) particle hopping or exchange in lattice models, or diffusive spreading in a continuum setting. Still within a mean-field framework that entails mass action factorization of non-linear correlations, in the continuous representation this leads to a *reaction-diffusion equation*

$$\frac{\partial a(\vec{x},t)}{\partial t} \approx \left(\sigma - \mu + D\nabla^2\right) a(\vec{x},t) - \bar{\lambda}\, a(\vec{x},t)^2 \tag{9}$$

for the *density field* $a(\vec{x},t)$ with diffusion constant $D > 0$. In the population dynamics context, this non-linear partial differential equation is referred to as the Fisher–Kolmogorov(–Petrovskii–Piskunov) equation.[3] In one spatial dimension, Eq. (9) admits solitary traveling wave solutions of the form $a(x,t) = u(x - c\,t)$ that interpolate between the active and inactive states, i.e., $u(z \to -\infty) = 0$, while $u(z \to \infty) = \bar{r} = (\sigma - \mu)/\bar{\lambda}$, if $\bar{r} > 0$; their detailed shape depends on the wave velocity c.

Away from the extinction threshold at $\sigma = \mu$, we may linearize this equation by considering the deviation $\delta a(\vec{x},t) = a(\vec{x},t) - a(\infty)$ from the asymptotic density $a(\infty)$. Upon neglecting quadratic terms in the fluctuations δa, one obtains near both the active (where $a(\infty) = \bar{r}$) and inactive states (with $a(\infty) = 0$)

$$\frac{\partial \delta a(\vec{x},t)}{\partial t} \approx \left(D\nabla^2 - |\sigma - \mu|\right) a(\vec{x},t)\ , \tag{10}$$

with characteristic length scale $\xi = \sqrt{D/|\sigma - \mu|}$ and corresponding time scale $\tau = \xi^2/D$ as to be expected for diffusive processes. The correlation length ξ describes the extent of spatially correlated regions, i.e., density clusters, in the system, whereas the rate $1/\tau$ governs their temporal decay.

Since $a(t) = \int a(\vec{x},t)\, d^d x$, the mean-field logistic equation (7) follows from Eq. (9) only under the assumption of extremely short-range spatial correlations $\sim \delta(\vec{x} - \vec{x}')$, i.e., in the limit $\xi \to 0$, which is definitely violated near the extinction threshold. This Dirac delta function also indicates that the non-linear reaction rate in the continuum description and the corresponding dimensionless mean-field rate are related to each other via the volume b^d of the unit cell in an ultimately underlying discrete lattice model: $\lambda \sim b^d\, \bar{\lambda}$. It is important to realize that the connection between microscopic reaction rates and their continuum counterparts is not usually direct and simple, but depends on the details of the involved coarse-graining process. With this caveat stated explicitly, which also applies to the relationship between lattice hopping rates and continuum diffusivities, we shall for notational simplicity henceforth drop the overbars from the continuum rates.

3.3. *Extinction threshold: directed percolation criticality*

On a lattice with N sites, where locally spontaneous particle death, reproduction, and binary coagulation (or annihilation) can take place, and which are coupled through particle hopping processes, the single-site extinction bifurcation discussed above translates into a genuine continuous non-equilibrium phase transition in the thermodynamic limit $N \to \infty$, or in the corresponding continuum model with infinitely many degrees of freedom. Note that in any finite stochastic system that incorporates an absorbing state, the latter is inevitably reached at sufficiently long times. A true absorbing-to-active phase transition hence requires taking the thermodynamic limit first in order to permit the existence of a stable active phase as $t \to \infty$. In addition, this asymptotic long-time limit must be considered prior to tuning any control parameters. Yet characteristic extinction times tend to grow exponentially with N and active states may survive in a quasi-stationary configuration as long as $\log t \ll \mathcal{O}(N)$. Hence absorbing phase transitions are in fact easily accessible numerically in computer simulations with sufficiently many lattice sites. As in the vicinity of critical points or second-order phase transitions in thermal equilibrium, non-linearities and fluctuations become crucial near the extinction threshold, and cannot be neglected in a proper mathematical treatment. Consequently, mean-field approximations that neglect both intrinsic reaction noise and spatial correlations become at least questionable.

The phenomenological description of active-to-absorbing (and other non-equilibrium) phase transitions closely follows that of near-equilibrium critical dynamics.[5,10–14] As the phase transition is approached upon tuning a relevant control parameter $r \to 0$, spatial correlations become drastically enhanced. For the correlation function of an appropriately chosen order parameter field that characterizes the phase transition (e.g., the particle density in our population dynamics model), one expects a typically algebraic divergence of the associated correlation length: $\xi(r) \sim |r|^{-\nu}$ with a critical exponent ν. Consequently, microscopic length (and time as well as energy) scales are rendered irrelevant, and the system asymptotically becomes scale-invariant. This emergent critical-point symmetry is reflected in power law behavior for various physical quantities that are captured through additional critical indices. The *dynamic critical exponent* z links the divergence of the characteristic relaxation time to that of the correlation length: $\tau(r) \sim \xi(r)^z \sim |r|^{-z\nu}$, describing *critical slowing-down*. The stationary (long-time) order parameter sets in algebraically: $a(t \to \infty, r) \sim r^{\beta}$

for $r > 0$, while it decays to zero as $a(t, r = 0) \sim t^{-\alpha}$ precisely at the critical point. These two power laws are limiting cases of a more general *dynamical scaling* ansatz for the time-dependent order parameter,

$$a(t, r) = |r|^{\beta}\, \hat{a}\big(t/\tau(r)\big) \ , \tag{11}$$

where the scaling function on the right-hand side satisfies $\hat{a}(0) = \text{const}$. For large arguments $y = t/\tau(r) \sim t\,|r|^{z\nu}$, one must require $\hat{a}(y) \sim y^{-\beta/z\nu}$ in order for the r dependence to cancel as $r \to 0$. Hence we obtain the critical decay exponent $\alpha = \beta/z\nu$. This *scaling relation* is of course fulfilled by the mean-field critical exponents $\alpha = \beta = 1$, $\nu = 1/2$, and $z = 2$ (indicating diffusive spreading) found in our previous population model analysis.

As for equilibrium critical phenomena, there exists an (upper) *critical dimension* d_c below which fluctuations are strong enough to modify not just amplitudes and scaling functions, but alter the critical scaling exponents. We invoke a simple scaling argumens to determine d_c for competing birth-death-coagulation processes: Let us set an inverse length (wave vector) scale κ, i.e., $[x] = \kappa^{-1}$, and corresponding time scale $[t] = [x]^2 = \kappa^{-2}$ (implying that we choose $[D] = \kappa^0$), where the square bracket indicates the scaling dimension. Eq. (9) then enforces $[\sigma] = [\mu] = [r] = \kappa^2$; moreover, $[a(\vec{x}, t)] = \kappa^d$ since a represents a density field in d spatial dimensions, whence we find $[\lambda] = \kappa^{2-d}$ for the coagulation (or annihilation) rate. Non-linear stochastic fluctuations that will affect particle propagation and (linear) extinction incorporate subsequent branching and coagulation processes, and hence scale like the rate product $[\sigma\,\lambda] = \kappa^{4-d}$. The critical dimension $d_c = 4$ indicates when this effective non-linear coupling becomes scale-invariant. For $d < d_c$, it attains a positive scaling dimension and is considered *relevant* (in the renormalization group sense), along with the 'mass'-like parameter r. In dimensions beyond d_c, the non-linearity becomes irrelevant and does not alter the fundamental scaling properties of the model, yet of course fluctuations still contribute numerically to various observables. At $d = d_c$, one usually finds *logarithmic corrections* to the mean-field power laws.[5,14]

In order to heuristically include fluctuations, one may add (for simplicity) Gaussian white noise with vanishing average $\langle \zeta(\vec{x}, t) \rangle = 0$ to the reaction-diffusion equation (9), turning it into a stochastic partial differential equation:[5,12]

$$\frac{\partial a(\vec{x}, t)}{\partial t} = \big(\lambda\, r + D\nabla^2\big)\, a(\vec{x}, t) - \lambda\, a(\vec{x}, t)^2 + \zeta(\vec{x}, t) \ . \tag{12}$$

Note that the deterministic part of the right-hand side can be interpreted as an expansion of a very general reaction functional in terms of the small

fluctuating local particle density near the extinction threshold, and even the diffusive spreading term may be viewed as the leading contribution in a long-wavelength expansion for spatially varying fluctuations (in systems with spatial inversion symmetry). Eq. (12) is thus quite generic, provided there are no additional special symmetries that would enforce the coefficients r or λ to vanish. For $r > 0$ and if $\lambda > 0$, the system resides in an active phase, whereas it reaches the empty, absorbing state for $r < 0$. For negative λ, one would have to amend Eq. (12) with a cubic term in the density field. The absence of a constant particle source (or sink) term on its right-hand side is mandated by presence of the absorbing state $a = 0$.

This constraint must be similarly reflected in the noise correlations: as the mean particle number $a(t) \to 0$, all stochastic fluctuations must cease. To lowest non-vanishing order in a, one would therefore posit

$$\langle \zeta(\vec{x}, t)\, \zeta(\vec{x}', t') \rangle = v\, a(\vec{x}, t)\, \delta(\vec{x} - \vec{x}') \delta(t - t') \ . \tag{13}$$

Stochastic dynamics with such a multiplicative noise correlator is properly defined through a corresponding functional integral representation;[5,12] intriguingly, the ensuing path integral action turns out to be equivalent to a well-studied problem in nuclear and particle physics, namely Reggeon field theory,[15] which in turn has been shown to capture the universal scaling properties of critical *directed percolation* clusters.[16,17] This sequence of mathematical mappings lends strong support to the Janssen–Grassberger conjecture,[17,18] which states that the asymptotic critical scaling features of continuous non-equilibrium transitions from active to inactive, absorbing states for a single scalar order parameter governed by Markovian stochastic dynamics, and in the absence of any quenched disorder and coupling to other conserved fields, should be described by the directed-percolation universality class. In fact, this statement applies generically even for multi-component systems.[19] Indeed, if we represent the basic stochastic death, birth, nearest-neighbor hopping, and coagulation processes on a lattice through their 'world lines' in a space-time plot as depicted in Fig. 1, it becomes apparent how they generate a directed percolation cluster.[12,14]

More rigorously, the Doi–Peliti formalism allows a representation of 'microscopic' stochastic reaction kinetics as defined through the associated master equation in terms of a coherent-state path integral.[5,13] For the combined reactions $A \to \emptyset$, $A \to A + A$, and $A + A \to A$ in the continuum limit, augmented with diffusive spreading, the resulting action assumes precisely the form of Reggeon field theory, and hence the 'mesoscopic' Langevin description (12, 13), in the vicinity of the absorbing-state transition.[5,12,13] As

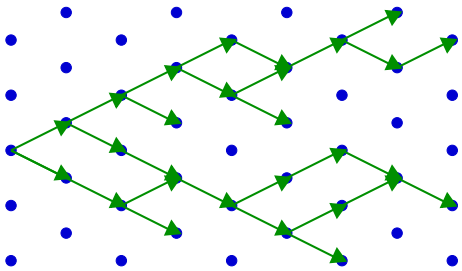

Fig. 1. Elementary death, birth, hopping, and coagulation processes initiated by a single particle seed generate a directed percolation cluster; bonds connecting lattice sites are formed only by advancing along the 'forward' (time-like) direction to the right. [Figure reproduced with permission from H. K. Janssen and U. C. Täuber, *Ann. Phys. (NY)* **315**, 147–192 (2005); DOI: 10.1016/j.aop.2004.09.011; copyright (2005) by Elsevier Inc.]

a consequence of a special internal 'rapidity reversal' symmetry of Reggeon field theory, the directed-percolation universality class is fully characterized by a set of only three independent critical exponents (say ν, z, and β); all other critical indices are related to them via exact scaling relations.

The critical exponents for directed percolation are known to high precision from dedicated Monte Carlo computer simulations;[10,11,14] recent literature values for α, β, ν, and z in two and three dimensions are listed in Table 1. For $d = 1$, the most accurate exponent values were actually obtained semi-analytically via ingenious series expansions.[20] A dynamical renormalization group analysis based on the (Reggeon) field theory representation allows a systematic perturbation expansion for the fluctuation corrections to the mean-field exponents in terms of the deviation $\epsilon = 4 - d$ from the critical dimension d_c.[5,12,13,15] The first-order (one-loop) results are also tabulated below; as compared to mean-field theory, critical fluctuations effectively reduce the values of $\alpha, \beta, 1/\nu$, and z in accord with the numerical data, and increasingly so for lower dimensions. Note that $z < 2$ implies sub-diffusive propagation at the extinction transition for $d < 4$. Several experiments have at least partially detected directed-percolation scaling near active-to-absorbing phase transitions in various systems.[14] Perhaps the most impressive confirmation originates from detailed and very careful studies of the transition between two different turbulent states of electrohydrodynamic convection in (quasi-)two-dimensional turbulent nematic liquid crystals carried out by Takeuchi et al. at the University of Tokyo,[21] who managed to extract twelve different critical exponents (four of them listed in Table 1) along with five scaling functions from their experimental data.

Table 1. Critical exponents for directed percolation obtained from series expansions in one dimension;[20] Monte Carlo simulations in two and three dimensions;[14] first-order perturbative renormalization group analysis ($d = 4 - \epsilon$);[12] and experiments on turbulent nematic liquid crystals ($d = 2$)[21] (numbers in brackets indicate last-digit uncertainties).

critical exponent	dimension $d = 1$	$d = 2$	$d = 3$	$d = 4 - \epsilon$	liquid crystal experiment
α	0.159464(6)	0.4505(10)	0.732(4)	$1 - \frac{\epsilon}{4} + \mathcal{O}(\epsilon^2)$	0.48(5)
β	0.276486(8)	0.5834(30)	0.813(9)	$1 - \frac{\epsilon}{6} + \mathcal{O}(\epsilon^2)$	0.59(4)
ν	1.096854(4)	0.7333(75)	0.584(5)	$\frac{1}{2} + \frac{\epsilon}{16} + \mathcal{O}(\epsilon^2)$	0.75(6)
z	1.580745(10)	1.7660(16)	1.901(5)	$2 - \frac{\epsilon}{12} + \mathcal{O}(\epsilon^2)$	1.72(11)

4. Dynamic Correlations in Pair Annihilation Processes

4.1. *Depletion zones and reaction rate renormalization*

We next return to simple pair annihilation ($A + A \to \emptyset$, rate λ') or fusion ($A + A \to A$, rate λ) processes, but in spatially extended systems. The on-site master equation for the former looks like Eq. (3), with the gain term replaced with $\lambda'\,(n+1)(n+2)\,P(n+2)$. This merely results in a rescaled reaction rate $\lambda \to 2\lambda'$ in both the exact Eq. (4) and the mean-field equations (5), (6). However, as the particle density drops toward substantial dilution, the rate of further pair annihilation processes will ultimately not be determined by the original microscopic reactivity λ (λ'), and instead be limited by the time it takes for two reactants to meet.[4,8,9,13] If we assume diffusive spreading with diffusion constant D, and hence relative diffusivity $2D$, the typical time for two particles at distance l to find each other is $t \sim l^2/4D$. In the diffusion-limited regime, l and t set the relevant length and time scales, whence the particle density should scale according to $a(t) \sim l(t)^{-d} \sim (D\,t)^{-d/2}$ in d spatial dimensions. This suggests a slower decay than the mean-field prediction $a(t) \sim (\lambda\,t)^{-1}$ in dimensions $d < 2$. Indeed, the previously established scaling dimension $[\lambda] = \kappa^{2-d}$ too indicates that $d_c = 2$ sets the critical dimension for diffusion-controlled pair annilation. In one dimension, the certain return of a random walker to its origin ensures that the ensuing annihilations carve out *depletion zones*, generating spatial *anti-correlations* that impede subsequent reactions. In contrast, for $d > 2$ diffusive spreading sustains a well-mixed system with largely homogeneous density, and mean-field theory remains valid.

This simple scaling argument is quantitatively borne out by Smoluchowski's classical self-consistent approach.[4,13] In a continuum representation, we need to impose a finite reaction sphere with radius b: two particles

react, once their distance becomes smaller than b. In a quasi-stationary limit, we then need to solve the stationary diffusion equation

$$0 = \nabla^2 a(r) = \frac{\partial^2 a(r)}{\partial r^2} + \frac{d-1}{r}\,\frac{\partial a(r)}{\partial r}\ , \tag{14}$$

where we have invoked spherical symmetry and written down the Laplacian differential operator in d-dimensional spherical coordinates. General solutions are then linear combinations of a constant term and the power r^{2-d}. For $d > 2$, we may impose the straightforward boundary conditions $a(r \le b) = 0$, whereas the particle density approaches a finite asymptotic value $a(\infty)$ far away from the reaction center located at the origin, which yields $a(r) = a(\infty)\left[1 - (b/r)^{d-2}\right]$. The effective reactivity $\widetilde{\lambda}$ in the diffusion-limited regime is then given by the incoming particle flux at reaction sphere boundary: $\widetilde{\lambda} \sim D b^{d-1} a(\infty)^{-1}\,[\partial a(r)/\partial r]\,|_{r=b} \sim D(d-2)b^{d-2}$, which replaces the annihilation rate λ in the rate equation (5). Consequently, one obtains the large-time density decay $a(t) \sim (D\,t)^{-1}$ with the same power law (6) as in the reaction-controlled region at large densities.

However, at $d_c = 2$ the effective reaction rate $\widetilde{\lambda}$ vanishes; indeed, in low dimensions $d < 2$ one needs to impose a different boundary condition $a(R) \approx a(\infty)$, where R denotes the mean particle separation: since the density $a(R) \sim R^{-d}$, one has $R(a) \sim a^{-1/d}$. The boundary condition hence depends on the actual density in the quasi-stationary limit, resulting in the profile $a(r) = a(\infty)\left[(r/b)^{2-d} - 1\right] / \left[(R/b)^{2-d} - 1\right]$. From the diffusive flux at the reaction sphere one obtains the effective reactivity $\widetilde{\lambda}(a) \sim D(2-d)b^{d-2}/[(R/b)^{2-d} - 1] \to \lambda_R\, a^{-1+2/d}$ as $a \to 0$ and $R \to \infty$, with a constant $\lambda_R \sim D$ (that again tends to zero as $d \to 2$). Upon self-consistently replacing λ with the density-dependent effective rate $\widetilde{\lambda}(a)$ in Eq. (5), we arrive at

$$\frac{\partial a(t)}{\partial t} \sim -\lambda_R\, a(t)^{1+2/d}\ . \tag{15}$$

It solution through variable separation yields the anticipated slower density decay and in turn the time dependence of the effective reaction rate:

$$a(t) \sim (D\,t)^{-d/2}\ , \quad \widetilde{\lambda}(t) \sim (D\,t)^{-1+d/2}\ . \tag{16}$$

At the critical dimension $d_c = 2$, one finds logarithmic slowing-down relative to the rate equation power law: $a(t) \sim (D\,t)^{-1} \ln(8D\,t/b^2)$.

Dynamical renormalization group calculations based on the Doi–Peliti field theory representation of the associated master equation confirm these findings.[5,13,22,23] For kth order annihilation $k\,A \to \emptyset, A, \ldots, (k-1)A$

($k \geq 2$) the right-hand side of Eq. (5) is to be replaced with $-\lambda_k\, a(t)^k$; for diffusive propagation, dimensional analysis then yields the scaling dimension $[\lambda_k] = \kappa^{2-(k-1)\,d}$, from which one infers the upper critical dimension $d_c(k) = 2/(k-1)$. Deviations from the mean-field algebraic decay $a(t) \sim t^{-1/(k-1)}$ should only materialize for pair ($k = 2$) reactions for $d \leq 2$, and for triplet annihilationat $d_c(3) = 1$. In accord with Smoluchowski's underlying assumption, diffusive spreading is not affected by the non-linear annihilation processes. The resulting perturbation expansion in λ_k can be summed to all orders, and indeed recovers Eq. (16) for pair annihilation, and the corresponding logarithmic scaling at the critical dimension, which for triplet reactions becomes $a(t) \sim \left[(D\,t)^{-1} \ln(D\,t)\right]^{1/2}$.

Pair annihilation dynamics on one-dimensional lattices with strict site exclusion can also be mapped onto non-Hermitean spin-1/2 Heisenberg models, permitting the extraction of remarkably rich non-trivial exact results.[24–27] The anomalous density decay induced by the self-generated depletion zones has been confirmed in several experiments on exciton recombination kinetics in effectively one-dimensional molecular systems. Particularly convincing are data obtained by Allam et al. at the University of Surrey in carbon nanotubes, who managed to explore the detailed crossover in the power laws from the reaction-controlled to the diffusion-limited regime (16) both in the exciton density decay and the reactivity.[28]

4.2. *Segregation in diffusive two-species annihilation*

Let us now investigate pair annihilation of particles of distinct species, $A+B \to \emptyset$, with reaction rate λ.[1,3–5] The crucial distinction to the previous situation is that alike particles do not react with each other. The associated exact time evolution as well as the coupled mean-field rate equations for the densities $a(t)$ and $b(t)$ are symmetric under species exchange $A \leftrightarrow B$,

$$\frac{\partial a(t)}{\partial t} = \frac{\partial b(t)}{\partial t} = -\lambda\, \langle [n_A\, n_B](t) \rangle \approx -\lambda\, a(t)\, b(t)\ , \tag{17}$$

and these binary reactions of course preserve the number difference $n_C = n_A - n_B = \text{const.}$, whence also $c(t) = a(t) - b(t) = c(0)$. One must now distinguish between two situations: If initially $n_A = n_B$ precisely, $c(t) = 0$ at all times: with identical initial conditions for their same rate equations, $a(t) = b(t)$. Eq. (17) consequently reduces to Eq. (5) for pair annihilation of identical species, with the solution (6) that describes algebraic decay to zero for both populations. In the more generic case $n_A \neq n_B$, say, with majority species A, i.e, $c(0) > 0$, the B population will asymptotically go

extinct, $b(\infty) = 0$, while $a(\infty) = c(0)$. At long times, we may thus replace $a(t) \approx c(0)$ in the rate equation for $b(t)$, resulting in exponential decay with time constant $c(0)\lambda$: $b(t) = a(t) - c(0) \sim e^{-c(0)\lambda\, t}$. The special symmetric case $c(0) = 0$ hence resembles a dynamical critical point with diverging relaxation time, and exponential density decay replaced by a power law.

In a spatial setting with diffusive transport, ultimately the stochastic pair annihilation reactions will become diffusion-limited, and the emerging depletion zones and persistent particle anti-correlations will markedly slow down the asymptotic decay of the minority species in low dimensions $d \leq d_c = 2$. Indeed, replacing $\lambda\, t \to \widetilde{\lambda}(t)\, t \sim (D\, t)^{d/2}$ with its renormalized counterpart according to Eq. (16), one arrives at stretched exponential behavior: $\ln b(t) = \ln[a(t) - c(0)] \sim -(D\, t)^{d/2}$ for $d < 2$, whereas $\ln b(t) = \ln[a(t) - c(0)] \sim -(D\, t)/\ln(D\, t)$ in two dimensions.

In the special symmetric case with equal initial particle numbers, the presence of an additional conserved quantity has a profound effect on the long-time chemical kinetics: Both particle species may spatially *segregate* into inert, slowly coarsening domains, whence the reactions become confined to the contact zones separating the A- or B-rich domains.[29,30] Note that the local particle density excess satisfies a simple diffusion equation $\partial c(\vec{x}, t)/\partial t = D\nabla^2 c(\vec{x}, t)$; the associated initial value problem is then solved by means of the diffusive Green's function $G(\vec{x}, t) = \Theta(t)\, e^{-\vec{x}^2/4D\, t}/4\pi D\, t$ via the convolution integral $c(\vec{x}, t) = \int G(\vec{x} - \vec{x}', t)\, c(\vec{x}', 0)\, d^d x'$. If one assumes an initially random, spatially uncorrelated Poisson distribution for both A and B particles with $\overline{a(\vec{x}, 0)} = \overline{b(\vec{x}, 0)} = a(0)$, where the overbar denotes an ensemble average over initial conditions, and $\overline{a(\vec{x}, 0)\, a(\vec{x}', 0)} = \overline{b(\vec{x}, 0)\, b(\vec{x}', 0)} = a(0)^2 + a(0)\, \delta(\vec{x} - \vec{x}')$, whereas $\overline{a(\vec{x}, 0)\, b(\vec{x}', 0)} = 0$, the corresponding moments for the initial density excess become $\overline{c(\vec{x}, 0)} = 0$ and $\overline{c(\vec{x}, 0)\, c(\vec{x}', 0)} = 2a(0)\, \delta(\vec{x} - \vec{x}')$.

These considerations allow us to explicitly evaluate

$$\overline{c(\vec{x}, t)^2} = 2\, a(0) \int G(\vec{x} - \vec{x}' t)^2\, d^d x' = \frac{2\, a(0)\, \Theta(t)}{(8\pi D\, t)^{d/2}} \tag{18}$$

through straightforward Gaussian integration. The distribution of the field c itself will be Gaussian as well, with zero mean and variance (18); hence we finally obtain for the average absolute value of the local density excess

$$\overline{|c(\vec{x}, t)|} = \sqrt{\frac{2}{\pi}\, \overline{c(\vec{x}, t)^2}} = \sqrt{\frac{4\, a(0)}{\pi}}\ \frac{\Theta(t)}{(8\pi D\, t)^{d/4}}\ . \tag{19}$$

In high dimensions $d > 4$, this excess decays faster than the mean densities $a(t) \sim 1/t$, implying that the particle distribution remains largely uniform,

and mean-field theory provides a satisfactory description. In contrast, for $d < d_s = 4$, the long-time behavior is dictated by the slowly decaying spatial density excess fluctuations: $a(t) \sim b(t) \sim (D\,t)^{-d/4}$. Either species accumulate in diffusively growing domains of linear size $l(t) \sim (D\,t)^{1/2}$ separated by active *reaction zones* whose width relative to $l(t)$ decreases algebraically with time.[31] Note that the borderline dimension for spatial species segregation $d_s = 4$ is not a critical dimension in the renormalization group sense; the anomalous density decay as consequence of segregated domain formation can rather be fully described within the framework of mean-field reaction-diffusion equations.[30] The resulting power law $a(t) \sim t^{-3/4}$ in three dimensions was experimentally observed in a calcium-fluorophore system by Monson and Kopelman at the University of Michigan.[32]

The above analysis does not apply to specific, spatially correlated initial conditions. For example, if impenetrable hard-core particles are aligned in strictly alternating order $\cdots ABABABA \cdots$ on a one-dimensional line, pair annihilation reactions will preserve this arrangement at all later times. Hence the distinction between the two species becomes in fact meaningless, and the single-species asymptotic decay $\sim (D\,t)^{-1/2}$ ensues. More generally, pair annilation processes involving q distinct species $A_i + A_j \to \emptyset$ $(1 \leq i < j \leq q)$ should eventually reduce to just a two-species system for the remaining two 'strongest' particle types, as determined by their reaction rates, diffusivities, and initial concentrations. Novel, distinct behavior could thus only appear for highly symmetric situations where all reaction and diffusion rates as well as initial densities are set equal among the q species.

Yet it turns out that for any $q \geq 3$ there exist no conserved quantities in such systems. One may furthermore establish the borderline dimension for species segregation as $d_s(q) = 4/(q-1)$; for $d \geq 2$, therefore all densities should follow the mean-field decay law $\sim 1/t$ as for a single species.[33] Only in one dimension can distinct particle species cluster into stable domains, resulting in a combination of depletion- and segregation-dominated decay:

$$a_i(t) \sim t^{-1/2} + C\,t^{-\alpha(q)} \ , \quad \alpha(q) = \frac{q-1}{2\,q} \ . \tag{20}$$

Note that $\alpha(2) = 1/4$ as established above, while the single-species decay exponent is recovered in the limit of infinitely many species, $\alpha(\infty) = 1/2$: In that situation, alike particles experience a vanishing probability to ever encounter each other, whence the distinction between the different species becomes irrelevant. Once again, correlated initial linear arrangements such as $\cdots ABCDABCD \cdots$ for four species induce special cases; here, no alike

particles can ever meet, and the system behaves effectively like single-species pair annihilation again. Also, interesting cyclic variants may be constructed,[34] such as $A+B \to \emptyset$, $B+C \to \emptyset$, $C+D \to \emptyset$, and $D+A \to \emptyset$. In this case, one may collect individuals from species A and C, and similarly B and D, in just two competing 'alliances', and consequently the decay kinetics is captured by the two-species pair annihilation behavior.

5. Stochastic Pattern Formation in Population Dynamics

5.1. *Activity fronts in predator-prey coexistence models*

The language and also numerical and mathematical tools developed for the investigation of chemical kinetics may be directly transferred to spatially extended stochastic population dynamics.[5,35,36] Aside from the logistic population growth with finite carrying capacity (7), another classical and paradigmatic model in ecology concerns the competition and coexistence of prey with their predator species, as first independently constructed by Lotka and Volterra.[1,3] Let B indicate the prey species, who left on their own merely undergo (asexual) reproduction $B \to B+B$ with rate σ. Their population is held in check by predators A who may either spontaneously die, $A \to \emptyset$ with rate μ, or upon encounter with a prey individual, devoure it and simultaneously generate offspring: $A + B \to A + A$ with rate λ. The original deterministic Lotka–Volterra model consists of the associated coupled mean-field rate equations for the population densities $a(t)$ and $b(t)$:

$$\frac{\partial a(t)}{\partial t} = -\mu\, a(t) + \lambda\, a(t)\, b(t)\ , \quad \frac{\partial b(t)}{\partial t} = \sigma\, b(t) - \lambda\, a(t)\, b(t)\ . \tag{21}$$

This dynamics allows three stationary states, namely (i) complete extinction $a = b = 0$; (ii) the also absorbing pure prey state with Malthusian population explosion $a = 0$, $b \to \infty$; and (iii) a predator-prey coexistence state with finite densities $a(\infty) = \sigma/\lambda$, $b(\infty) = \mu/\lambda$. Naturally, the predators benefit from high prey fertility σ, while the prey prosper if the predators are short-lived; yet counter-intuitively for the predators, both stationary population numbers decrease with enhanced predation rates λ, signaling a non-linear feedback mechanism: If the A species too efficiently reduces the B population, they have scarce food left, whence the majority of them die.

However, this stationary coexistence state (iii) is in fact never reached under the deterministic non-linear dynamics (21). Indeed, eliminating time through taking the ratio $da/db = (\lambda\, b - \mu)\, a/\,(\sigma - \lambda\, a)\, b$, one obtains after variable separation and integration a *conserved first integral* for the

mean-field dynamics: $K(t) = \lambda\,[a(t) + b(t)] - \sigma \ln a(t) - \mu \ln b(t) = K(0)$. The trajectories in the phase space spanned by the population numbers must therefore be strictly periodic orbits, implying undamped non-linear population oscillations whose amplitudes and shapes are fixed by the initial values $a(0)$ and $b(0)$. For small deviations from the stationary coexistence center $\delta a(t) = a(t) - a(\infty)$, $\delta b(t) = b(t) - b(\infty)$, straightforward linearization of Eqs. (21) yields $\partial \delta a(t)/\partial t \approx \sigma\,\delta b(t)$, $\partial \delta b(t)/\partial t \approx -\mu\,\delta a(t)$, which are then readily combined to the simple harmonic oscillator differential equation $\partial^2 \delta a(t)/\partial t^2 \approx -\omega^2\,a(t)$ with (linear) oscillation frequency $\omega = \sqrt{\mu\,\sigma}$. Equivalently, we may construct the linear stability matrix $\mathbf{L}$ that governs the temporal evolution of the fluctuation vector $\mathbf{v} = (\delta a\ \delta b)^T$: $\partial \mathbf{v}(t)/\partial t \approx \mathbf{L}\,\mathbf{v}(t)$, where $\mathbf{L} = \begin{pmatrix} 0 & \sigma \\ -\mu & 0 \end{pmatrix}$ with imaginary eigenvalues $\pm i\omega$.

Clearly the absence of any real part in the stability matrix eigenvalues represents a degenerate, a-typical situation that should not be robust against even minor modifications of the model.[3] For example, in order to render the Lotka–Volterra description more realistic and prevent any population divergence, one could impose a finite carrying capacity r for species B; at the mean-field level, this alters the second differential equation in (21) to

$$\frac{\partial b(t)}{\partial t} = \sigma\,b(t)\,[1 - b(t)/r] - \lambda\,a(t)\,b(t)\ , \tag{22}$$

leading to modified stationary states (ii') $a(\infty) = 0$, $b(\infty) = r$ and (iii') $a(\infty) = \sigma\,(1 - \mu/\lambda\,r)\,/\lambda$, $b(\infty) = \mu/\lambda$. The latter two-species coexistence fixed point exist, and is linearly stable, provided the predation rate exceeds the threshold $\lambda_c = \mu/r$; for $\lambda < \lambda_c$, the predator species A is driven to extinction. At the stationary state (iii'), the linear stability matrix eigenvalues acquire negative real parts:

$$\epsilon_\pm = -\frac{\mu\,\sigma}{2\,\lambda\,r}\left[1 \pm \sqrt{1 - \frac{4\,\lambda\,r}{\sigma}\left(\frac{\lambda\,r}{\mu} - 1\right)}\right]\ , \tag{23}$$

For $\sigma > 4\,\lambda\,r\,(\lambda\,r/\mu - 1)$, these eigenvalues are both real, indicating exponential relaxation towards the stable node (iii'). For lower prey birth rates, trajectories in phase space spiral inwards to reach the stationary state (iii') which now represents a stable focus, and the imaginary part of $\epsilon_\pm$ gives the frequency of the resulting damped population oscillations. One may amend this mean-field description to allow for spatial structures by replacing the population numbers with local density fields and adding diffusion terms as

in Eq. (9). In one dimension, the ensuing coupled set of partial differential equations permits traveling wave solutions which describe predator invasion fronts originating in a region set in the coexistence state (iii') and moving into space occupied only by prey.[3]

Monte Carlo computer simulations with sufficiently large populations display rich dynamical features in the (quasi-)stable predator-prey coexistence regime that reflect the mean-field picture only partially.[35–37] Already in a local 'urn' model without spatial degrees of freedom, intrinsic fluctuations, often termed demographic noise in this context, dominate the dynamics and induce persistent stochastic population oscillations. These can be understood through the effect of white-noise driving on a damped oscillator: On occasion, the stochastic forcing will hit the oscillator's eigenfrequency, and via this resonant amplification displace the phase space trajectories away from the stable coexistence fixed point.[38]

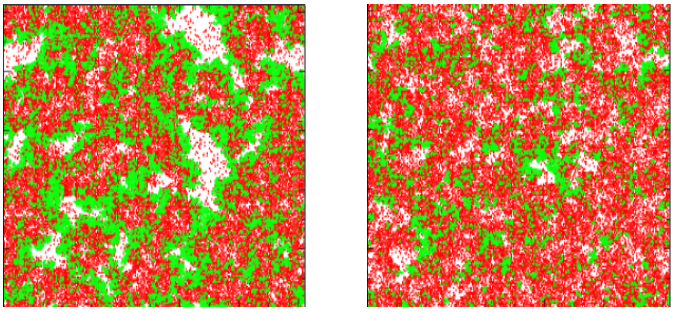

(a) (b)

Fig. 2. Snapshots of a stochastic Lotka–Volterra model on a square lattice with 256×256 sites, periodic boundary conditions, site occupation number exclusion, and random initial particle placement after (a) 500; (b) 1000 Monte Carlo steps. Sites occupied by predators are color-coded in red, by prey in green, and empty spaces in white. [Figures reproduced with permission from S. Chen and U. C. Täuber, *Phys. Biol.* **13**, 025005-1–11 (2016); DOI: 10.1088/1478-3975/13/2/025005; copyright (2016) by IOP Publ.]

In stochastic Lotka–Volterra models on a lattice that permit an arbitrary number of particles per site, nearest-neighbor hopping transport generates wave-like propagation of these erratic local population oscillations.[37] As depicted in the two-dimensional simulation snapshots of Fig. 2, prey may thus invade empty regions, followed by predators who feed on them, and in turn re-generate space devoid of particles in their wake. Surviving prey islands then act as randomly placed sources of new activity fronts; it

is hence the very stochastic nature of the kinetics that both causes and stabilizes these intriguing spatio-temporal patterns.[39,40] They are moreover quite robust with respect to modification of the microscopic model implementations, and are invariably observed in the predator-prey coexistence phase in two and three dimensions, even when the Lotka–Volterra process $A+B \to A+A$ is separated into independent predation and predator birth reactions,[41] or if at most a single particle is allowed on each lattice site. For large predation rates, one observes very distinct and prominent activity fronts; for smaller values of λ, closer to the extinction threshold, instead there appear confined fluctuating predator clusters immersed in a sea of abundant prey. These two different types of structures may be related to the distinct properties of the mean-field linear stability matrix: Real eigenvalues $\epsilon_{\pm}$ that indicate purely relaxational kinetics correspond to isolated prey clusters in the spatial system, whereas imaginary parts in Eq. (23) associated with spiraling trajectories and damped oscillations pertain to spreading predator-prey fronts.

In either case, analysis of the Fourier-transformed average population densities quantitatively establishes that stochastic fluctuations both drastically renormalize the oscillation frequencies relative to the rate equation prediction and generate attenuation.[35,37] Based on the Doi–Peliti mapping of the corresponding master equation to a continuum field theory,[5,13] a perturbative computation in terms of the predation rate λ qualitatively confirms these numerical observations: It demonstrates the emergence of a noise-induced effective damping, as well as the fluctuation-driven instability towards spatially inhomogeneous structures in dimensions $d \leq 4$; the calculation also explains the strong downward renormalization for the population oscillation frequency as caused by an almost massless mode.[42]

Implementing a finite local carrying capacity through constraining the site lattice occupations, say, to at most a single particle of either type, in addition produces an extinction threshold for the predator species as in the mean-field rate equation (22). As one should indeed expect on general grounds,[19] this continuous active-to-absorbing phase transition is governed by the directed-percolation universality class. This fact can be established formally by starting from the Doi–Peliti action, and reducing it to Reggeon field theory near the predator extinction threshold.[35,42] Heuristically, the prey population almost fills the entire lattice in this situation; consequently, the presence of B particles sets no constraint on the predation process $A+B \to A+A$, which reduces to the branching reaction $A+A \to A$. Along with predator death $A \to \emptyset$ and the population-limiting pair fusion reaction

$A + A \to A$ that is in fact equivalent to local site occupation restrictions, one recovers the fundamental processes of directed percolation. Extensive Monte Carlo simulations confirm directed-percolation critical exponents at the predator extinction transition,[35,36,43] including the associated critical aging scaling behavior for the two-time density auto-correlations.[5,44]

5.2. *Clusters and spiral patterns in cyclic competition games*

Extension of two-species models to systems with multiple reactants in general increases the complexity of the problem tremendously.[36] Nevertheless, simpler sub-structures can be amenable to full theoretical analysis. For example, on occasion elementary competition cycles are present in food networks. As a final illustration of the often decisive role of spatial correlations in stochastic chemical reactions or population dynamics, we therefore consider the following cyclic interaction scheme involving three species subject to Lotka–Volterra predation: $A+B \to A+A$ with rate λ_A; $B+C \to B+B$ with rate λ_B; and $A + C \to C + C$ with rate λ_C, akin to the rock-paper-scissors game.[2] These elementary replacement processes conserve the total particle number $N = N_A+N_B+N_C$ and hence density $\rho = a(t)+b(t)+c(t)$; of course this is also true on the level of the coupled rate equations

$$\frac{\partial a(t)}{\partial t} = a(t)\,[\lambda_A\, b(t) - \lambda_C\, c(t)]\ , \quad \frac{\partial b(t)}{\partial t} = b(t)\,[\lambda_B\, c(t) - \lambda_A\, a(t)]\ ,$$
$$\frac{\partial c(t)}{\partial t} = c(t)\,[\lambda_B\, a(t) - \lambda_B\, b(t)]\ ; \tag{24}$$

aside from the three absorbing states $(a, b, c) = (\rho, 0, 0)$, $(0, \rho, 0)$, and $(0, 0, \rho)$, which are linearly unstable under the mean-field dynamics (24), yet represent the sole possible final configurations in any finite stochastic realization, there exists one neutrally stable reactive coexistence state: $a(\infty) = \rho\,\lambda_B/(\lambda_A + \lambda_B + \lambda_C)$, $b(\infty) = \rho\,\lambda_C/(\lambda_A + \lambda_B + \lambda_C)$, $c(\infty) = \rho\,\lambda_A/(\lambda_A + \lambda_B + \lambda_C)$. The linear stability matrix at this fixed point reads

$$\mathbf{L} = \frac{\rho}{\lambda_A + \lambda_B + \lambda_C} \begin{pmatrix} 0 & \lambda_A\,\lambda_B & -\lambda_B\,\lambda_C \\ -\lambda_A\,\lambda_C & 0 & \lambda_B\,\lambda_C \\ \lambda_A\,\lambda_C & -\lambda_A\,\lambda_B & 0 \end{pmatrix};$$

one of its eigenvalues is zero reflecting the conservation law ρ =const., the other two are purely imaginary, $\epsilon_\pm = \pm i\rho\,\sqrt{\lambda_A\,\lambda_B\,\lambda_C/(\lambda_A + \lambda_B + \lambda_C)}$, indicating undamped population oscillations.

Akin to the Lotka–Volterra two-species competition model discussed previously, one might thus anticipate traveling wave structures. Yet Monte

Carlo simulations of this rock-papers-scissors model on two-dimensional lattices that are sufficiently large to prevent extinction events and stabilize the three-species coexistence state, one merely observes weakly fluctuating clusters containing particles of the same type,[45,46] as shown in Fig. 3(a). Upon initializing the system with a random spatial distribution, transient population oscillations appear, with a characteristic frequency that differs considerably from the mean-field prediction, but they are strongly damped, at variance with the results from the rate equation analysis. These findings are perhaps even more curious given in light of the fact that in the extreme asymmetric limit $\lambda_A \gg \lambda_B, \lambda_C$, the rock-paper-scissors system effectively reduces to the Lotka–Volterra model with predators A, prey B, and abundant, essentially saturated C population with $c(\infty) \approx \rho$. Indeed, on the mean-field level, one finds to leading order $a(\infty) \approx \rho\,\lambda_B/\lambda_A$, $b(\infty) \approx \rho\,\lambda_C/\lambda_A$, and $c(\infty) \approx \rho\,[1 - (\lambda_B + \lambda_C)/\lambda_A]$. We may thus replace $c(t) \approx \rho$ in the rate equations (24), which takes us to Eq. (21) with effective predator death rate $\mu = c(\infty)\,\lambda_C$ and prey reproduction rate $\sigma = c(\infty)\,\lambda_B$. Lattice simulations of strongly asymmetric rock-paper-scissors model display the characteristic Lotka–Volterra spreading activitiy fronts and persistent oscillatory kinetics, and hence confirm this picture.[47]

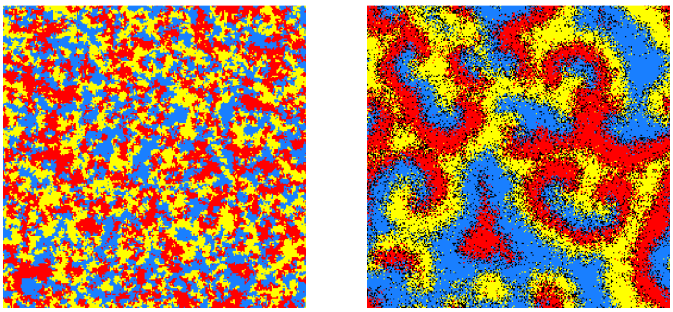

(a) (b)

Fig. 3. Snapshots of a stochastic cyclic competition models on square lattices with 256×256 sites, periodic boundary conditions, site occupation number exclusion, and random initial particle placement: (a) cyclic Lotka–Volterra or rock-paper-scissors model with conserved total particle number; (b) May–Leonard model with separate predation and reproduction processes. Sites occupied by A, B, and C particles are respectively color-coded in red, yellow, and blue; empty spaces in black. [Figures reproduced with permission from (a) Q. He, M. Mobilia, and U. C. Täuber, *Phys. Rev. E* **82**, 051909-1–11 (2010); DOI: 10.1103/PhysRevE.82.051909; copyright (2010) by The American Physical Society; (b) Q. He, M. Mobilia, and U. C. Täuber, *Eur. Phys. J. B* **82**, 97–105 (2011); DOI: 10.1140/epjb/e2011-20259-x; copyright (2011) by EDP Sciences.]

In the May–Leonard model variant of cyclic competition, predation and birth reactions are explicitly separated: $A+B \to A$, $A \to A+A$ (and cyclically permuted) with independent rates.[2] In this coupled reaction scheme, the total particle number is not conserved anymore, but still permits an active three-species coexistence state. In the absence of intra-species competition, i.e., for infinite carrying capacities, one eigenvalue of the associated linear stability matrix $\mathbf{L}$ is real and negative, corresponding to an exponentially relaxing mode. The other two eigenvalues are purely imaginary, signifying the existence of undamped oscillations. Monte Carlo simulations of the May–Leonard model on two-dimensional lattices show the spontaneous formation of spiral patterns with alternating A, B, C species in sequence.[36,45,48] These spiral structures become especially clear and pronounced if in addition to nearest-neighbor hopping, particle exchange $A \leftrightarrow B$ etc. is implemented, as illustrated in Fig. 3(b).[49]

On the mean-field rate equation level, one may argue the relaxing eigenmode to be irrelevant for the long-time dynamics of this system; confining the subsequent analysis to the reactive plane spanned by the remaining oscillating modes, a mapping to the complex Ginzburg–Landau equation has been achieved,[50] which is known to permit spiral spatio-temporal structures in certain parameter regimes.[51] A consistent treatment of intrinsic reaction noise for this model based again on the Doi–Peliti formalism however results in a more complex picture. Since the relaxing mode is randomly driven by non-linear fluctuations that involve the persistent oscillatory eigenmodes, it can only be integrated out in a rather restricted parameter range that allows for distinct time scale separation. In general, therefore the May–Leonard model is aptly described by a coupled set of three Langevin equations with properly constructed multiplicative noise.[52]

6. Summary and Concluding Remarks

In this chapter, we have given an overview over crucial fluctuation and correlation effects in simple spatially extended particle reaction systems that originate from the underlying stochastic kinetics; these very same models also pertain to the basic phenomenology for infectious disease spreading in epidemiology and the dynamics of competing populations in ecology. As befits the theme of this volume, the essential dynamical features of the paradigmatic models discussed here require analysis beyond the standard textbook fare that mostly utilizes coupled deterministic rate equations, which entail a factorization of correlation functions into powers of the reac-

tants' densities, thereby neglecting both temporal and spatial fluctuations.

Spontaneous death-birth reactions augmented with population-limiting fusion constitute the fundamental simple epidemic process. The ensuing population extinction threshold exemplifies a continuous non-equilibrium phase transition between active and absorbing states which is naturally governed by large and long-range fluctuations. It is generically characterized by the critical scaling exponents of directed percolation, which assume non-trivial values in dimensions below the upper critical dimension $d_c = 4$.

Binary (or triplet) annihilation reactions generate depletion zones in dimensions $d \leq d_c = 2$ (1); the particle anti-correlations cause a drastic slowing-down of the reaction kinetics in the diffusion-limited regime. For pair annihilation involving two distinct species, spatial segregation in dimensions $d \leq d_s = 4$ confines the reactions to the interfaces separating the diffusively coarsening domains. In the special case of precisely equal species densities, this further diminishes the overall reaction activity, and considerably decelerates the asymptotic algebraic decay.

In stochastic, spatially extended variants of the classical Lotka–Volterra model for predator-prey competition, the intrinsic demographic noise causes and stabilizes spreading activity fronts in the species coexistence phase; their quantitative properties are strongly affected by the stochastic fluctuations and spatial correlations self-generated by the fundamental reaction kinetics in the system. Furthermore, the implementation of finite local carrying capacities for the prey population, mimicking limitations in their food resources, generates an extinction threshold for the predator species. Finally, we have elucidated some basic features in cyclic competition models that involve three particle species, and related the resulting spatial structures, i.e., population clusters for direct rock-paper-scissors competition and dynamical spirals in the May–Leonard model, to the presence and absence, respectively, of a conservation law for the total particle number.

In more complex systems that involve a larger number of reactants, many of these fluctuation-dominated features may of course be effectively averaged out or become inconspicuous on relevant length and/or time scales. However, even when important qualitative properties such as the topology of the phase diagram or the essential functional form of the time evolution remain adequately captured by mean-field rate equations, internal fluctuations as well as emerging spatial and temporal patterns or even short-lived correlations may well drastically modify the numerical values of effective reaction rates and transport coefficients.

Two case studies from the author's research group may illustrate this

point: (I) In ligand-receptor binding kinetics on cell membranes or surface plasmon resonance devices that are commonly utilized to measure reaction affinities, repeated ligand rebinding to nearby receptor locations entails temporal correlations that persist under diffusive dynamics and even advective flow; the correct reaction rate values may consequently deviate drastically from numbers extracted by inadequate fits to straightforward rate equation kinetics.[53] (II) Circularly spreading wave fronts of 'killer' as well as resistant bacteria strains induce the formation of intriguing patterns in an effectively two-dimensional synthetic *E. coli* micro-ecological system, emphasizing the important role of spatial inhomogeneities and local correlations.[54] A sound understanding of the potential effects of fluctuations and correlations is thus indispensable for proper theoretical modeling and analysis as well as quantitative interpretation of experimental data.

There are of course other crucial fluctuation and correlation effects on chemical reactions and population dynamics that could not be covered in this chapter.[36] Prominent examples are the strong impact of intrinsic noise on extinction probabilities and pathways in finite systems;[55] and novel phenomena related to extrinsic random influences or quenched internal disorder.[56] These topics and many more are addressed elsewhere in this book.

Acknowledgments

I would like to sincerely thank my collaborators over the past 25 years for their invaluable insights and crucial contributions to our joint research on stochastic reaction-diffusion and population dynamics, especially: Timo Aspelmeier, Nicholas Butzin, John Cardy, Jacob Carroll, Sheng Chen, Udaya Sree Datla, Oliviér Deloubrière, Ulrich Dobramysl, Kim Forsten-Williams, Erwin Frey, Ivan Georgiev, Yadin Goldschmidt, Manoj Gopalakrishnan, Qian He, Bassel Heiba, Henk Hilhorst, Haye Hinrichsen, Martin Howard, Hannes Janssen, Weigang Liu, Jerôme Magnin, William Mather, Mauro Mobilia, Michel Pleimling, Matthew Raum, Beth Reid, Gunter Schütz, Franz Schwabl (deceased), Shannon Serrao, Steffen Trimper, Ben Vollmayr-Lee, Mark Washenberger, Frédéric van Wijland, and Royce Zia.

This research was in part sponsored by the US Army Research Office and was accomplished under Grant Number W911NF-17-1-0156. The views and conclusions contained in this document are those of the author and should not be interpreted as representing the official policies, either expressed or implied, of the Army Research Office or the US Government. The US Government is authorized to reproduce and distribute reprints for

Government purposes notwithstanding any copyright notation herein.

References

1. H. Haken, *Synergetics*. Springer, Berlin (1983).
2. J. Hofbauer and K. Sigmund, *Evolutionary games and population dynamics*. Cambridge University Press, Cambridge (1998).
3. J. D. Murray, *Mathematical biology*, Vols. I & II. Springer, New York, 3rd. ed. (2002).
4. P. K. Krapivsky, S. Redner, and E. Ben-Naim, *A kinetic view of statistical physics*. Cambridge University Press, Cambridge (2010).
5. U. C. Täuber, *Critical dynamics – A field theory approach to equilibrium and non-equilibrium scaling behavior*. Cambridge University Press, Cambridge (2014).
6. N. G. van Kampen, *Stochastic processes in physics and chemistry*. North Holland, Amsterdam (1981).
7. C. M. van Vliet, *Equilibrium and non-equilibrium statistical mechanics*. World Scientific, New Jersey, 2nd. ed. (2010).
8. V. Kuzovkov and E. Kotomin, Kinetics of bimolecular reactions in condensed media: Critical phenomena and microscopic self-organisation, *Rep. Prog. Phys.* **51**, 1479–1523 (1988).
9. A. A. Ovchinnikov, S. F. Timashev, and A. A. Belyy, *Kinetics of diffusion-controlled chemical processes*. Nova Science, New York (1989).
10. H. Hinrichsen, Nonequilibrium critical phenomena and phase transitions into absorbing states, *Adv. Phys.* **49**, 815–958 (2001).
11. G. Ódor, Phase transition universality classes of classical, nonequilibrium systems, *Rev. Mod. Phys.* **76**, 663–724 (2004).
12. H. K. Janssen and U. C. Täuber, The field theory approach to percolation processes, *Ann. Phys. (NY).* **315**, 147–192 (2005).
13. U. C. Täuber, M. J. Howard, and B. P. Vollmayr-Lee, Applications of field-theoretic renormalization group methods to reaction-diffusion problems, *J. Phys. A: Math. Gen.* **38**, R79–R131 (2005).
14. M. Henkel, H. Hinrichsen, and S. Lübeck, *Non-equilibrium phase transitions*, Vol. 1: *Absorbing phase transitions*. Springer, Dordrecht (2008).
15. M. Moshe, Recent developments in Reggeon field theory, *Phys. Rep.* **37**, 255–345 (1978).
16. J. L. Cardy and R. L. Sugar, Directed percolation and Reggeon field theory, *J. Phys. A: Math. Gen.* **13**, L423–L427 (1980).
17. H. K. Janssen, On the nonequilibrium phase transition in reaction-diffusion systems with an absorbing stationary state, *Z. Phys. B Cond. Matt.* **42**, 151–154 (1981).
18. P. Grassberger, On phase transitions in Schlögl's second model, *Z. Phys. B Cond. Matt.* **47**, 365–374 (1982).
19. H. K. Janssen, Directed percolation with colors and flavors, *J. Stat. Phys.* **103**, 801–839 (2001).

20. I. Jensen, Low-density series expansions for directed percolation on square and triangular lattices, *J. Phys. A: Math. Gen.* **29**, 7013–7040 (1996).
21. K. A. Takeuchi, M. Kuroda, H. Chaté, and M. Sano, Experimental realization of directed percolation criticality in turbulent liquid crystals, *Phys. Rev. E* **80**, 051116-1–12 (2009).
22. L. Peliti, Renormalisation of fluctuation effects in the $A + A \to A$ reaction, *J. Phys. A: Math. Gen.* **19**, L365–367 (1986).
23. B. P. Lee, Renormalization group calculation for the reaction $kA \to \emptyset$, *J. Phys. A: Math. Gen.* **27**, 2633–2652 (1994).
24. F. C. Alcaraz, M. Droz, M. Henkel, and V. Rittenberg, Reaction-diffusion processes, critical dynamics, and quantum chains, *Ann. Phys. (NY)* **230**, 250–302 (1994).
25. M. Henkel, E. Orlandini, and J. Santos, Reaction-diffusion processes from equivalent integrable quantum chains, *Ann. Phys. (NY)* **259**, 163–231 (1997).
26. G. M. Schütz, Exactly solvable models for many-body systems far from equilibrium, in: *Phase transitions and critical phenomena*, Vol. 19, eds. C. Domb and J. L. Lebowitz, Academic Press, London (2001).
27. R. Stinchcombe, Stochastic nonequilibrium systems, *Adv. Phys.* **50**, 431–496 (2001).
28. J. Allam, M. T. Sajjad, R. Sutton, K. Litvinenko, Z. Wang, S. Siddique, Q.-H. Yang, W. H. Lo, and T. Brown, Measurement of a reaction-diffusion crossover in exciton-exciton recombination inside carbon nanotubes using femtosecond optical absorption, *Phys. Rev. Lett.* **111**, 197401-1–5 (2013).
29. D. Toussaint and F. Wilczek, Particle-antiparticle annihilation in diffusive motion, *J. Chem. Phys.* **78**, 2642–2647 (1983).
30. B. P. Lee and J. Cardy, Renormalization group study of the $A + B \to \emptyset$ diffusion-limited reaction, *J. Stat. Phys.* **80**, 971–1007 (1995).
31. B. P. Lee and J. Cardy, Scaling of reaction zones in the $A + B \to \emptyset$ diffusion-limited reaction, *Phys. Rev. E* **50**, R3287–R3290 (1994).
32. E. Monson and R. Kopelman, Nonclassical kinetics of an elementary $A+B \to C$ reaction-diffusion system showing effects of a speckled initial reactant distribution and eventual self-segregation: experiments, *Phys. Rev. E* **69**, 021103-1–12 (2004).
33. H. J. Hilhorst, O. Deloubrière, M. J. Washenberger, and U. C. Täuber, Segregation in diffusion-limited multispecies pair annihilation, *J. Phys. A: Math. Gen.* **37**, 7063–7093 (2004).
34. H. J. Hilhorst, M. J. Washenberger, and U. C. Täuber, Symmetry and species segregation in diffusion-limited pair annihilation, *J. Stat. Mech.* P10002-1–19 (2004).
35. M. Mobilia, I. T. Georgiev, and U. C. Täuber, Phase transitions and spatio-temporal fluctuations in stochastic lattice Lotka–Volterra models, *J. Stat. Phys.* **128**, 447–483 (2007).
36. U. Dobramysl, M. Mobilia, M. Pleimling, and U. C. Täuber, Stochastic population dynamics in spatially extended predator-prey systems, *J. Phys. A: Math. Theor.* **51**, 063001-1–49 (2018).
37. M. J. Washenberger, M. Mobilia, and U. C. Täuber, Influence of local carry-

ing capacity restrictions on stochastic predator-prey models, *J. Phys. Cond. Matt.* **19**, 065139-1–14 (2007).
38. A. J. McKane and T. J. Newman, Predator-prey cycles from resonant amplification of demographic stochasticity, *Phys. Rev. Lett.* **94**, 218102-1–5 (2005).
39. T. Butler and N. Goldenfeld, Robust ecological pattern formation induced by demographic noise, *Phys. Rev. E* **80**, 030902(R) -1–4 (2009).
40. T. Butler and N. Goldenfeld, Fluctuation-driven Turing patterns, *Phys. Rev. E* **84**, 011112 -1–12 (2011).
41. M. Mobilia, I. T. Georgiev, and U. C. Täuber, Fluctuations and correlations in lattice models for predator-prey interaction, *Phys. Rev. E* **73**, 040903(R)-1–4 (2006).
42. U. C. Täuber, Population oscillations in spatial stochastic Lotka–Volterra models: A field-theoretic perturbational analysis, *J. Phys. A: Math. Theor.* **45**, 405002-1–34 (2012).
43. S. Chen and U. C. Täuber, Non-equilibrium relaxation in a stochastic lattice Lotka–Volterra model, *Phys. Biol.* **13**, 025005-1–11 (2016).
44. M. Henkel and M. Pleimling, *Non-equilibrium phase transitions*, Vol. 2: *Ageing and dynamical scaling far from equilibrium*. Springer, Dordrecht (2010).
45. M. Peltomäki and M. Alava, Three-and four-state rock-paper-scissors games with diffusion. *Phys. Rev. E* **78**, 031906-1–7 (2008).
46. Q. He, M. Mobilia, and U. C. Täuber, Spatial rock-paper-scissors models with inhomogeneous reaction rates, *Phys. Rev. E* **82**, 051909-1–11 (2010).
47. Q. He, U. C. Täuber, and R. K. P. Zia, On the relationship between cyclic and hierarchical three-species predator-prey systems and the two-species Lotka–Volterra model, *Eur. Phys. J. B* **85**, 141-1–13 (2012).
48. T. Reichenbach, M. Mobilia, and E. Frey, Mobility promotes and jeopardizes biodiversity in rock-paper-scissors games, *Nature* **448**, 1046–1049 (2007).
49. Q. He, M. Mobilia, and U. C. Täuber, Coexistence in the two-dimensional May–Leonard model with random rates, *Eur. Phys. J. B* **82**, 97–105 (2011).
50. T. Reichenbach, M. Mobilia, and E. Frey, Self-organization of mobile populations in cyclic competititon, *J. Theor. Biol.* **254**, 368–383 (2008).
51. I. S. Aranson and L. Kramer, The world of the complex Ginzburg–Landau equation, *Rev. Mod. Phys.* **74**, 99–144 (2002).
52. S. R. Serrao and U .C. Täuber, A stochastic analysis of the spatially extended May–Leonard model, *J. Phys. A: Math. Theor.* **50**, 404005-1–16 (2017).
53. J. Carroll, M. Raum, K. Forsten-Williams, and U. C. Täuber, Ligand-receptor binding kinetics in surface plasmon resonance cells: a Monte Carlo analysis, *Phys. Biol.* **13**, 066010-1–12 (2016).
54. U. S. Datla, W. H. Mather, S. Chen, I. W. Shoultz, U. C. Täuber, C. N. Jones, and N. C. Butzin, The spatiotemporal system dynamics of acquired resistance in an engineered microecology, *Scient. Rep.* **7**, 16071-1–9 (2017).
55. M. Assaf and B. Meerson, WKB theory of large deviations in stochastic populations, *J. Phys. A: Math. Theor.* **50**, 263001-1–63 (2017).
56. T. Vojta, Rare region effects at classical, quantum and nonequilibrium phase transitions, *J. Phys. A: Math. Gen.* **39**, R143–205 (2006).